

Supporting Information for

Polyphenol-mediated assembly of peptide for engineering

functional materials

Kaizhi Wang,^{‡a} Lingjun Sha,^{‡a} Minghui Wang,^b Yanbing Wu,^a Jianyang Lu,^a Yiwei Han,^a Chenbo Ji,^{*cd} Jie Yang^{*a} and Genxi Li^{*ac}

^aState Key Laboratory of Pharmaceutical Biotechnology, School of Life Sciences, Nanjing University, Nanjing 210023, P. R. China

^bJiangsu Co-Innovation Center of Efficient Processing and Utilization of Forest Resources, College of Science, Nanjing Forestry University, Nanjing, 210037, P. R. China

^cDepartment of Gynecology, Women's Hospital of Nanjing Medical University, Nanjing Women and Children's Healthcare Hospital, Nanjing 210004, P. R. China

^dNanjing Maternal and Child Health Institute, Women's Hospital of Nanjing Medical University, Nanjing Women and Children's Healthcare Hospital, Nanjing 210004, P. R. China

^eCenter for Molecular Recognition and Biosensing, School of Life Sciences, Shanghai University, Shanghai 200444, PR China

*Corresponding authors. E-mail addresses: chenboji@njmu.edu.cn (C. Ji); yangjie@nju.edu.cn (J. Yang); genxili@nju.edu.cn (G. Li).

[‡]These authors contributed equally to this work.

Experimental Section

Materials and Reagents

Tannic acid (TA), propyl gallate (PG), ellagic acid (EA), gallic acid (GA), epigallocatechin gallate (EGCG), and catechin (CAT) were purchased from Macklin Biochemical Technology Co. Ltd (Shanghai, China). All peptides (purity $\geq 95\%$) were chemically synthesized as lyophilized powders using the standard solid phase method. The peptide sequences are listed in Table S1. Branch peptide BR4G5 was synthesized by Hefei Scierbio Co., Ltd (China). All other peptides were synthesized by GenScript Biotech Co. Ltd (Nanjing China). Horseradish Peroxidase (HRP), Cytochrome C (CYC), 3,3',5,5'-tetramethylbenzidine (TMB), streptavidin (SA) were purchased from Aladdin Reagent (Shanghai) Co., Ltd. SA-RBITC, human immunoglobulin G (IgG), antifade mounting medium (with DAPI) and biotin-labeled HRP (HRP-Bio) were purchased from Solarbio Science & Technology Co. Ltd. (Beijing, China). Amplex Red (AR), bovine serum albumin (BSA), Tween-20, fetal bovine serum (FBS), 100 \times penicillin-streptomycin solution, and 4% paraformaldehyde fix solution were purchased from Shanghai Beyotime Biotechnology Co., Ltd (China). AntiCD44-FITC and mAb-HRP were purchased from Sino Biological Technology Co., Ltd. (Beijing, China). Glucose oxidase (GOx) and glucose were purchased from Sigma-Aldrich (Shanghai, China). BSA-FITC, IgG-FITC, FITC coupling kit, dimethyl sulfoxide (DMSO), and DMEM medium were purchased from Shanghai Sangon Biotechnology Co., Ltd (China). NaOH, NaCl, H₂O₂, HCl, Na₂CO₃, and NaHCO₃ were purchased from Nanjing Chemical Reagent Co., Ltd (China). All chemicals and reagents are analytical grade and used without further purification. Ultrapure water used in all experiments was prepared by the Milli-Q system (18.2 M Ω ·cm).

Apparatus

Transmission electron microscopy (TEM) images were taken from JEM 1200 EX (JEOL, Japan). The UV-vis spectra were recorded using a UV-2450 spectrophotometer (SHIMADZU, Japan). The fluorescence spectra were recorded using an FL-7000 fluorescence spectrophotometer (HITACHI, Japan). Dynamic light scattering (DLS)

and zeta potential of samples were conducted on Zetasizer Nano ZSE (Malvern, UK). Optical and fluorescence microscope images were pictured by inverted fluorescence microscope IX73 (Olympus, Japan). Confocal laser scanning microscopy (CLSM) images were acquired with Zeiss LSM880.

Results and Discussion

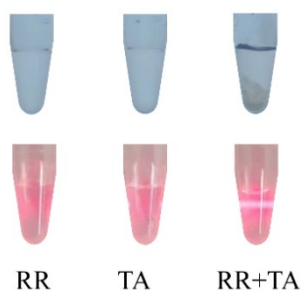


Fig. S1. Optical photographs of RR and TA alone versus a mixture of RR and TA.

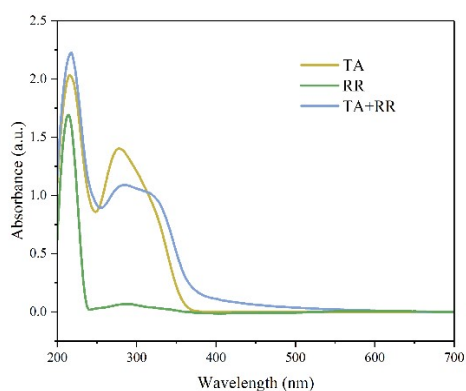


Fig. S2. UV-vis absorption spectra of RR, TA, and mixture of RR and TA.

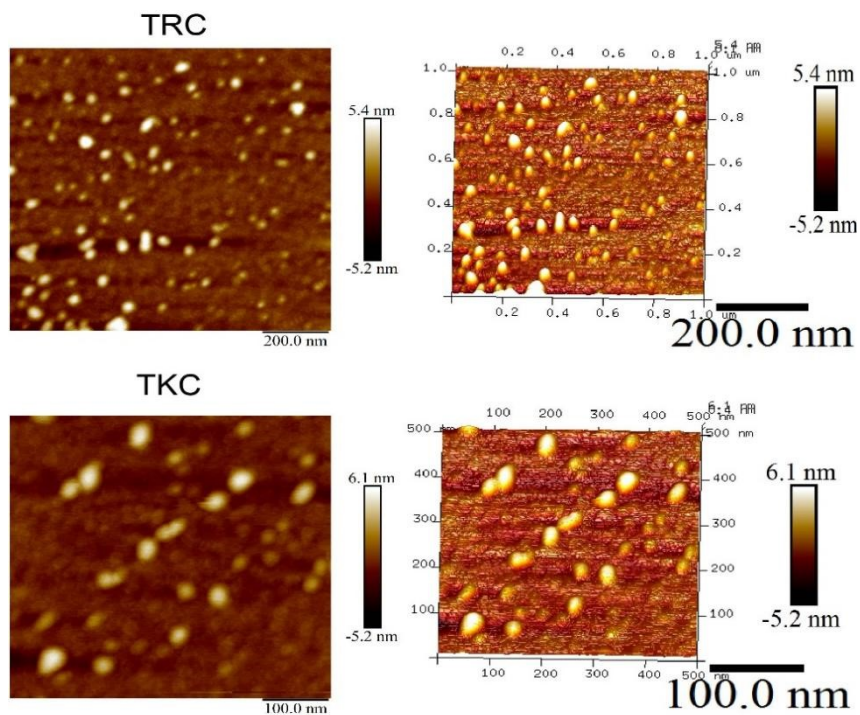


Fig. S3. AFM images of TRC and TKC.

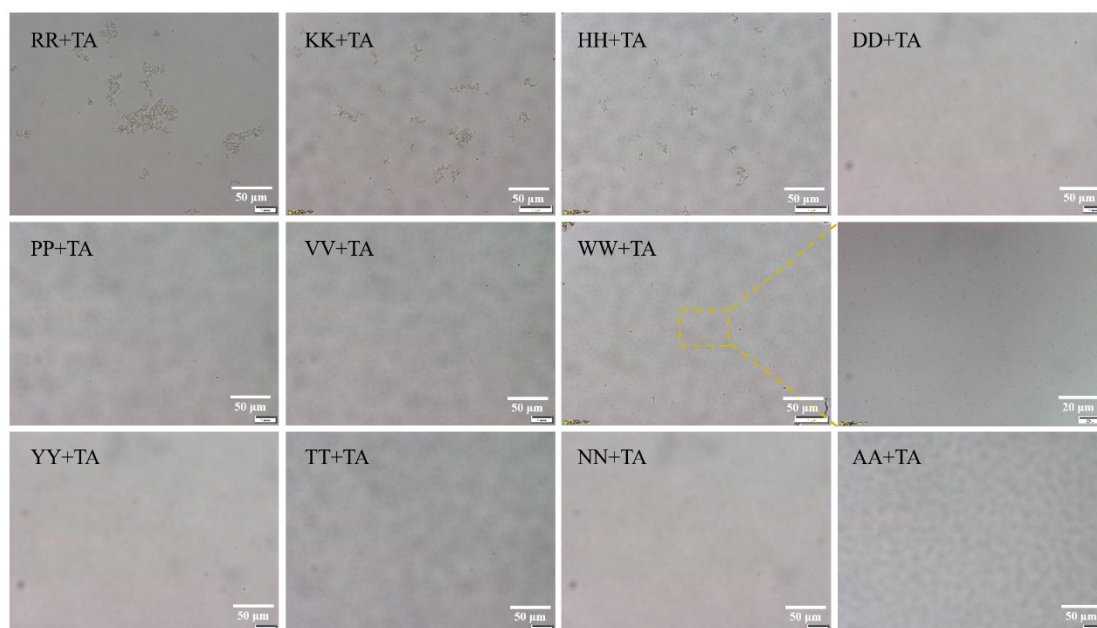


Fig. S4. Optical microscope images of various peptides mixed with TA in PBS (scale bars are 50 μm).

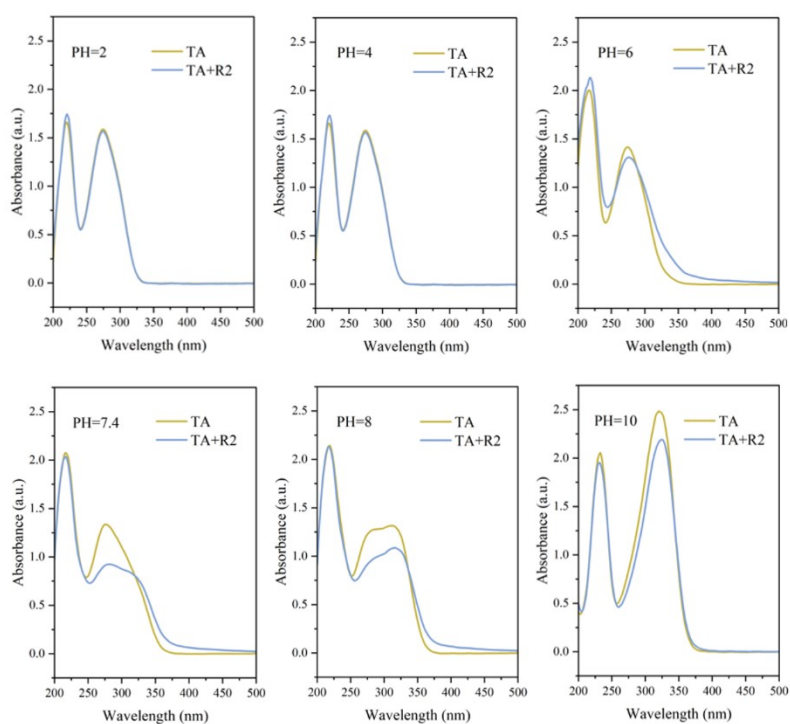


Fig. S5. UV-Vis absorption spectra of TA, TA+RR at different pH conditions.

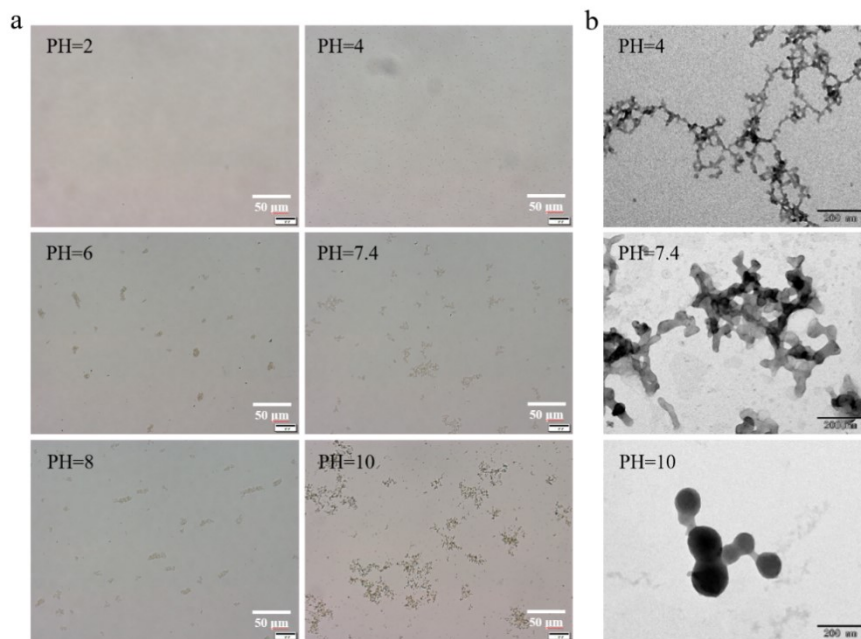


Fig. S6. Optical microscopy images (scale bars are 50 μm) (a) and TEM images of PPA at different pH conditions (scale bars are 200 nm).

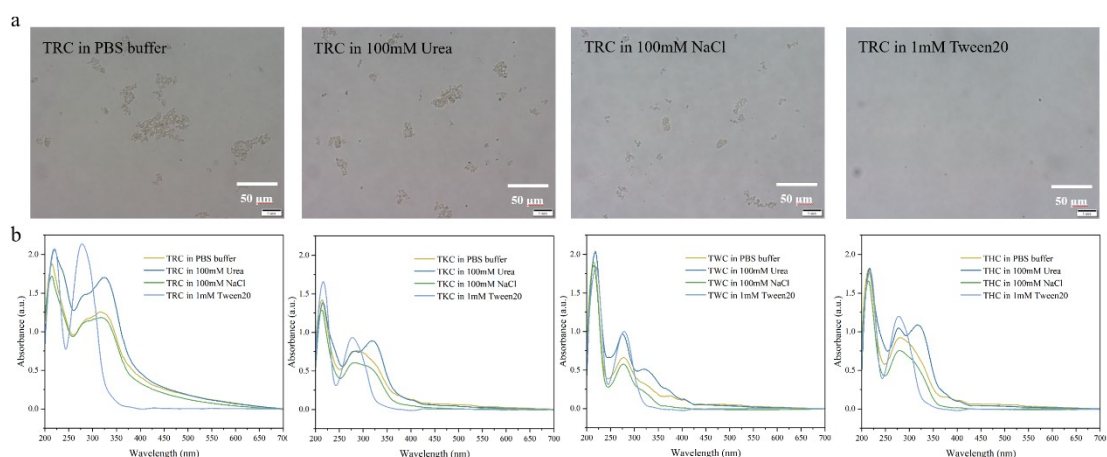


Fig. S7. a) Optical microscopy images of TRC after resuspension in PBS, Urea, NaCl, and Tween 20 (scale bars are 50 μm). b) UV-Vis absorption spectra of TRC, TKC, THC, and TWC after resuspension in PBS, Urea, NaCl, and Tween 20.

PH	2	4	6	7.4	8	10
PG						
GA						
EA						
CAT						
EGCG						

Fig. S8. Tyndall phenomenon of PG, EA, GA, EGCG, CAT mixed with RR at different pH conditions.

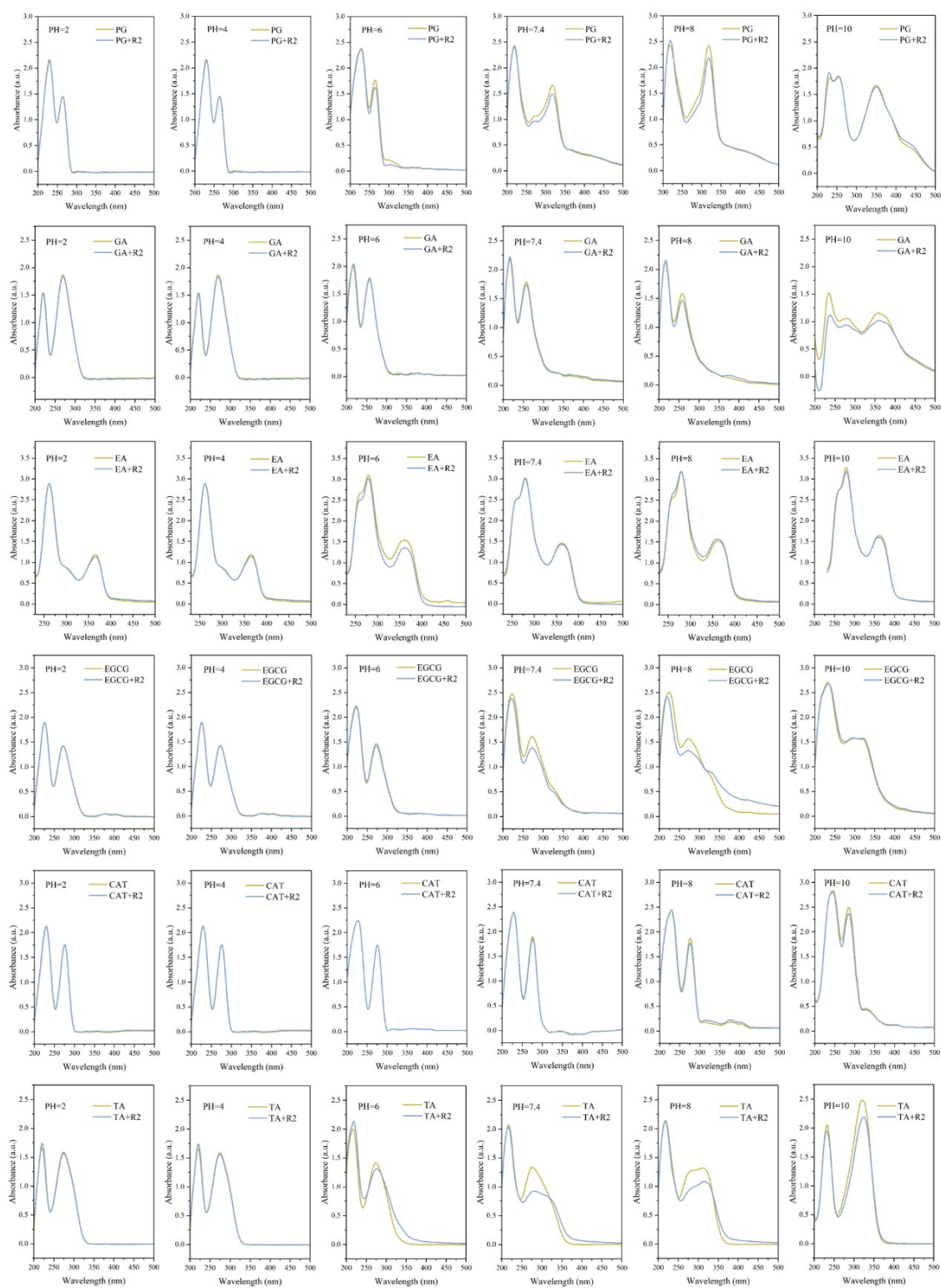


Fig. S9. UV-Vis absorption spectra of PG, EA, GA, EGCG, CAT, and their mixture with RR at different pH conditions.

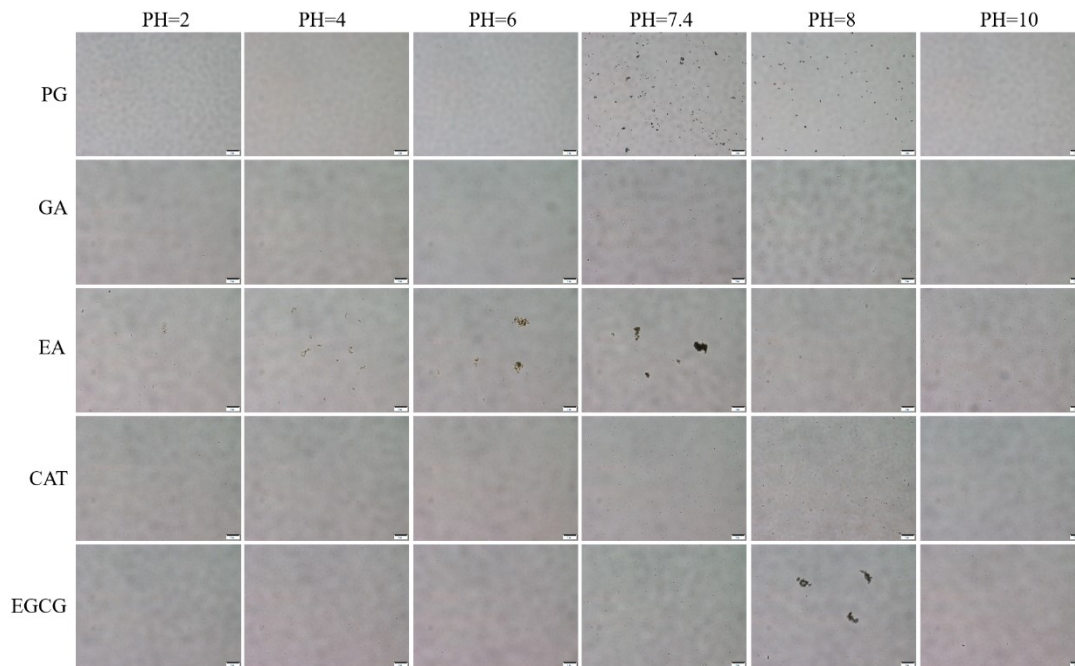


Fig. S10. Optical microscope images of PG, EA, GA, EGCG, and CAT mixed with RR at different pH conditions (scale bars are 100 μm).

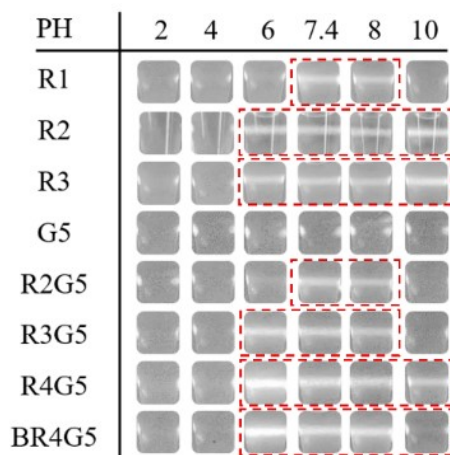


Fig. S11. Tyndall phenomenon of various peptides mixed with TA at various pH conditions.

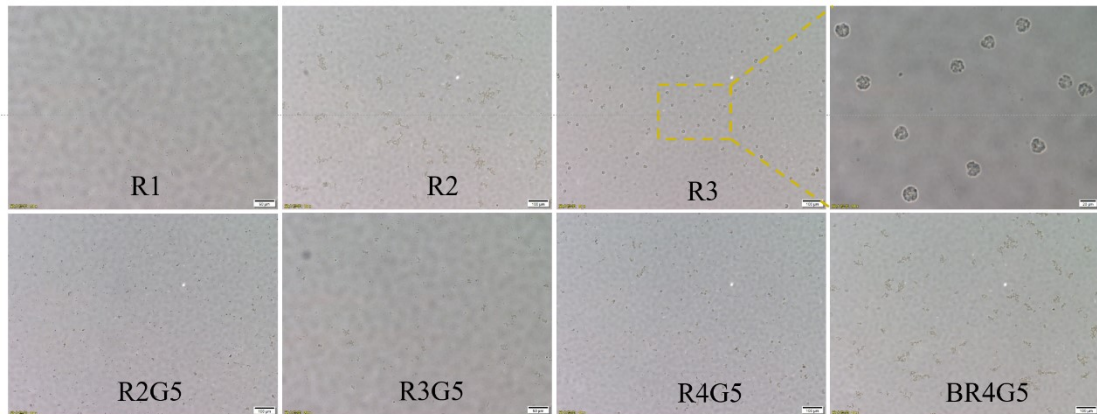


Fig. S12. Optical microscope images of assemblies of various peptides and TA (scale bars are 100 μm).

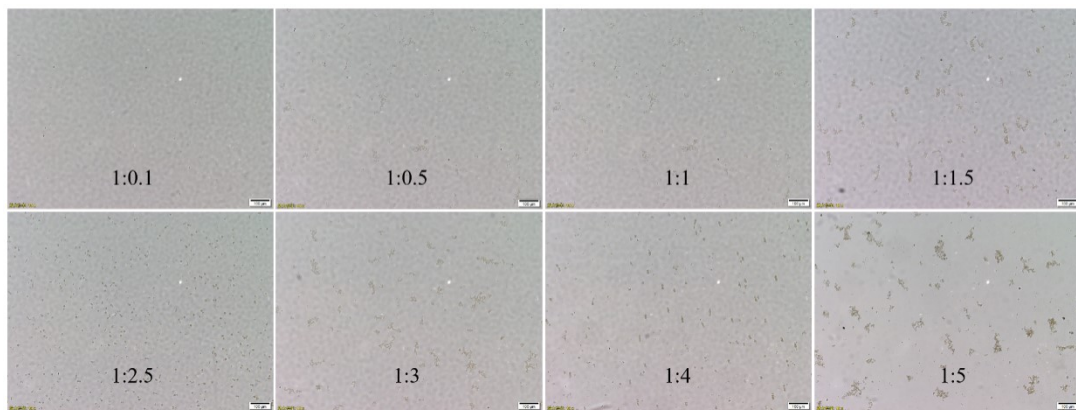


Fig. S13. Optical microscope image of TA mixed with RR in each ratio (scale bars are 100 μm).

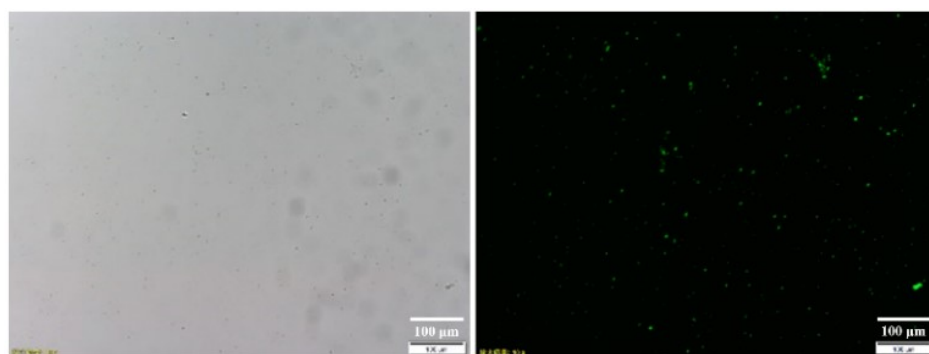


Fig. S14. Fluorescence microscopy images of PPAs@IgG-FITC (scale bars are 100 μm).

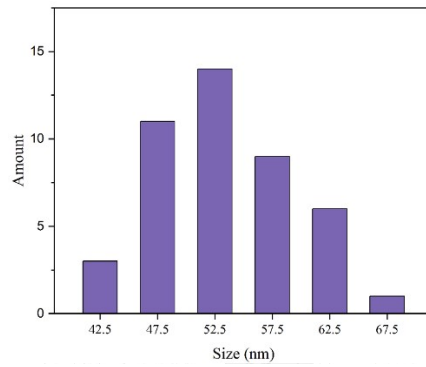


Fig. S15. Size distribution of PPAs@IgG.

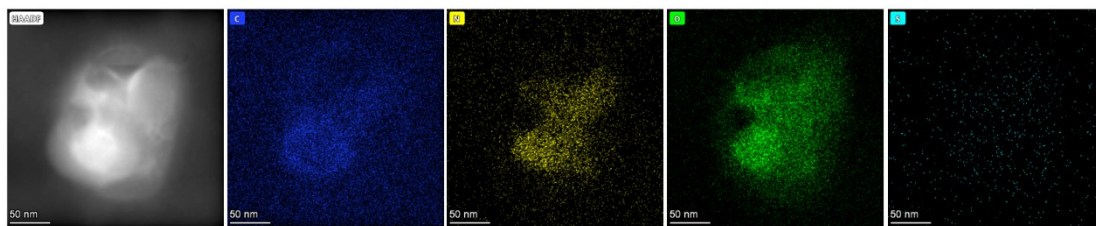


Fig. S16. EDS mapping of PPA@IgG (scale bars are 50 nm).

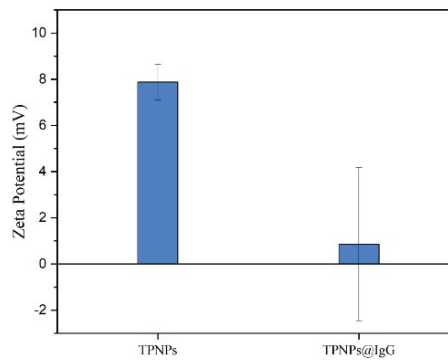


Fig. S17. Potential of PPAs and PPAs@IgG.

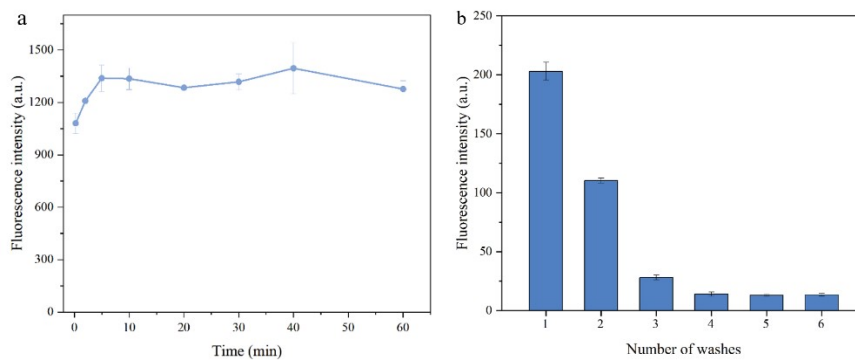


Fig. S18. a) Optimization of time for PPAs loading proteins. b) Optimization of the number of washes for PPAs loading proteins.

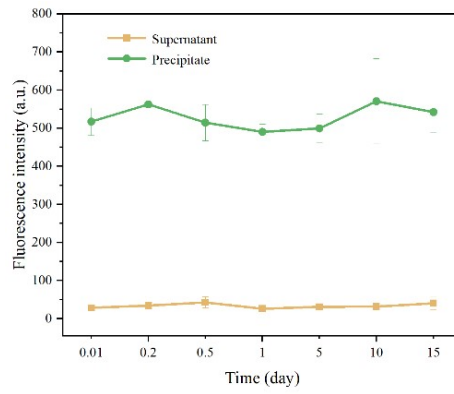


Fig. S19. Stability of proteins loaded on PPAs.

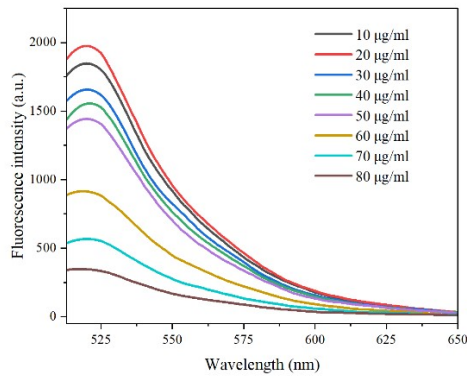


Fig. S20. The ability of PPAs to load IgG-FITC.

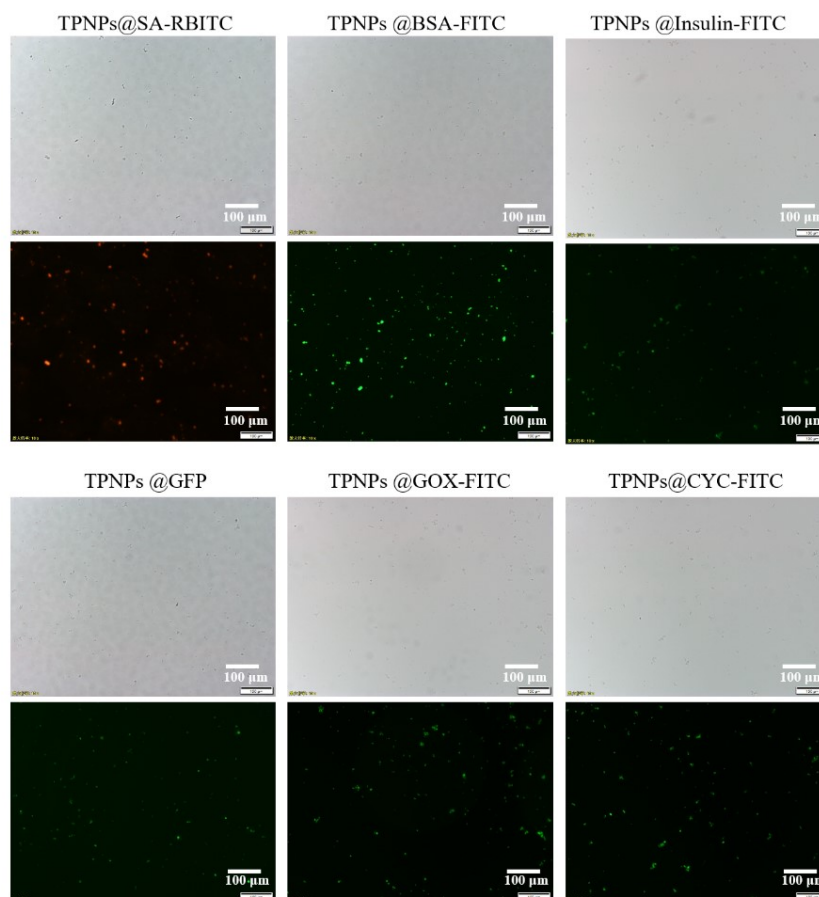


Fig. S21. Fluorescence microscopy images of various proteins loaded on PPAs (scale bars are 100 μm).

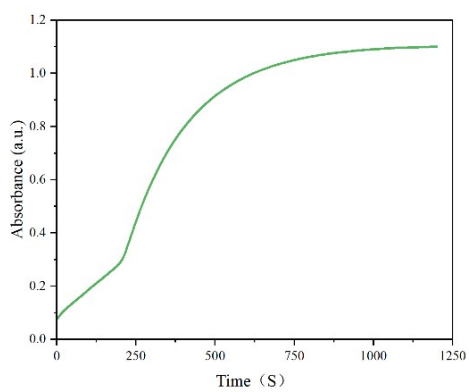


Fig. S22. Enzyme kinetic curve of PPAs@HRP.

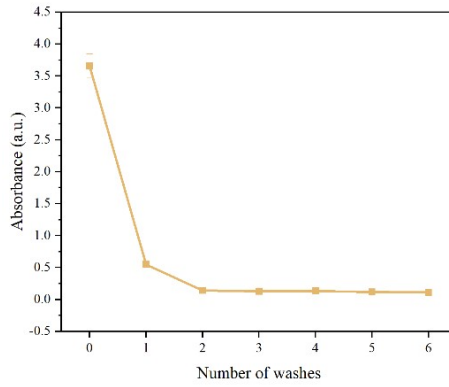


Fig. S23. Stability of mAb-HRP bound on PPAs@IgG.

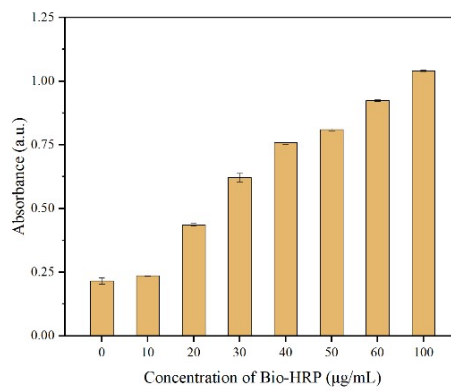


Fig. S24. Relationship between the amount of Bio-HRP bound on PPA@SA and its concentration.

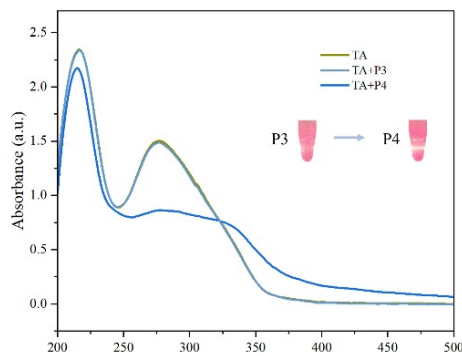


Fig. S25. UV-Vis absorption spectra of TA and P1, P2 mixing with TA. Inset: Tyndall phenomenon of P1, P2 mixed with TA.

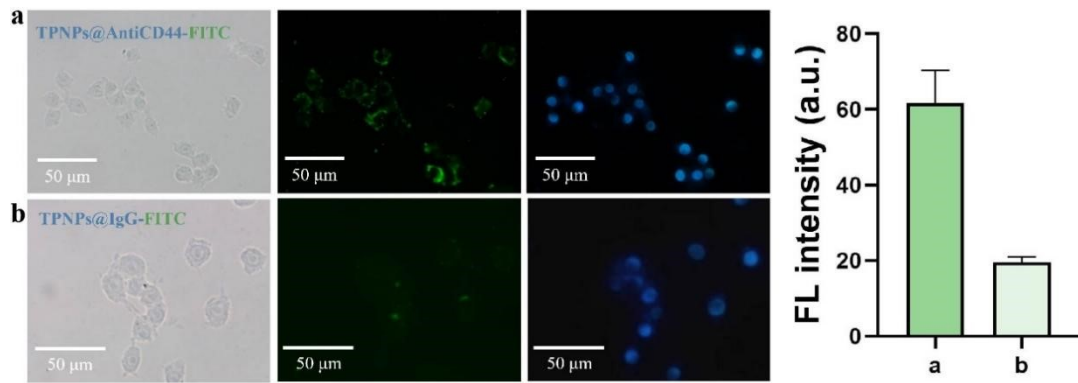


Fig. S26. Fluorescence microscopy images and fluorescence intensities of MDA-MB-231 after incubation 3 h with PPNPs@AntiCD44-FITC@BSA, PPNPs@IgG-FITC@BSA (scale bars are 50 μm).

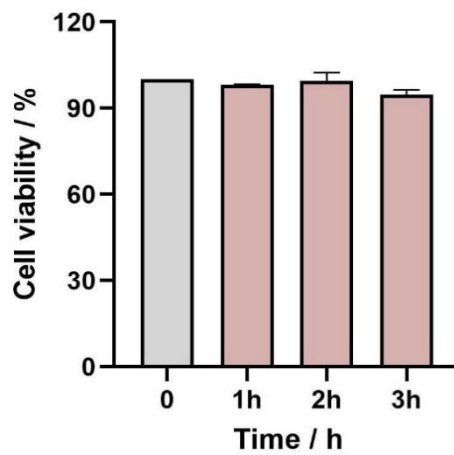


Fig. S27. Cell viability of MDA-MB-231 cells treated with PPNPs@BSA for different times.

Table S1. Sequences of all peptides used in this work.

Name	Sequence (N-terminal to C-terminal)
RR/R2	RRGGGRR
KK	KKGGGKK
HH	HHGGGHH
DD	DDGGGDD
PP	PPGGGPP
VV	VVGGGVV
WW	WWGGGWW
YY	YYGGGY
PP	PPGGGPP
VV	VVGGGVV
AA	AAGGGAA
R1	RGGGR
R3	RRRGGGRRR
G5	GGGGG
R2G5	RRGGGGG
R3G5	RRRGGGGG
R4G5	RRRRGGGGG
BR4G5	(RR) ₂ KGGGGG
P1	KTCENLADTY
P2	KTCENLADTYRRR
P3	ACSAG
P4	ACSAGRRR

Table S2. Molecular weight, isoelectric point, and aliphatic index of different proteins

Name	Molecular Weight (kDa)	Isoelectric Point (pI)	Aliphatic Index
GOx	131.28	4.2	86.12
Insulin	5.741	5.3	80.2
GFP	26.886	5.8	74.87
HRP	38.825	7.2	90.34
IgG	144.263	8.5	67.64
CYC	11.703	9.4	58.57
BSA	69.293	4.6	77.46
SA	65	6	63.4